

Extraction, Analysis and Interpretation of Digital Ionograms

A. Bartlett, M. Gallagher & M. Darnell

Hull-Lancaster Communications Research Group, UK

ABSTRACT

A digital ionogram is constructed from the impulse responses of sampled channels. If each sampled channel is processed in isolation, random channel noise is often interpreted as a true propagation mode. To overcome this problem, several adjacent channels can be processed together. The improvement of the impulse response and displayed ionogram by the application of median filters and low pass spatial filters is presented.

INTRODUCTION

The digital ionograms used for this research are created by the digital signal processing (DSP) of a received linear frequency modulation (LFM) or "chirp" transmission. In this sounding scheme the carrier signal is swept across a given band, typically the complete HF band, in a specific time interval [1]. The DSP based "chirp" monitoring system [2] samples a 3kHz channel, at given frequency intervals, over the whole of the HF band, using a standard HF radio receiver and a personal computer containing a DSP board. The digital ionograms are constructed from in a vertical raster of impulse responses from each sampled channel. The vertical axis represents relative time delay (ms) and horizontal axis represents frequency (2MHz to 30MHz).

In this system each channel impulse response is a discrete measurement which is used to form a representation of the modal structure of the ionosphere, along an oblique path. The channel impulse response is produced by quadrature matched filtering a digital representation of the 3kHz "chirp" waveform against a sampled received. A windowing function is applied to the digital "chirp" representation to reduce sidelobes produced by spectral leakage [3].

In order to resolve the position of the impulse response, which represent modes of propagation, only the apexes of the peaks are plotted on the digital ionogram. The peak detection algorithm rejects insignificant peaks by discounting peak amplitudes below a soft decision noise threshold, calculated for each channel.

WINDOW FUNCTIONS

The choice of windowing function has important implications on the matched filter performance. Channel impulse responses may have one or more peaks with differing amplitudes which correspond to

propagation modes. The choice of window function affects the following impulse response characteristics:

- (i) Resolution between peaks (before they merge into one). i.e. half power pulse width.
- (ii) The usable dynamic range for peak detection. i.e. peak-to-sidelobe ratio.
- (ii) The noise sensitivity of the matched filter. i.e. coherent gain.

The performance of the following windowing functions [4] have been evaluated for the quadrature matched filtering with band-limited AWGN; although it is realised that noise in HF channel is not Gaussian, the use of AWGN is a useful first stage in the evaluation process.

where N = correlation length.

$W[n]$ = the window n th tap multiplier value.

Rectangular Window (1)

$$W[n] = \begin{cases} 1 & 0 \leq n \leq (N-1) \\ 0 & \text{elsewhere} \end{cases}$$

Hamming Window (2)

$$W[n] = \begin{cases} 0.54 + 0.46 \cos\left(\frac{2n\pi}{N}\right) & 0 \leq n \leq (N-1) \\ 0 & \text{elsewhere} \end{cases}$$

Blackman Window (3)

$$W[n] = \begin{cases} 0.42 + 0.5 \cos\left(\frac{2n\pi}{N}\right) + 0.08 \cos\left(\frac{4n\pi}{N}\right) & 0 \leq n \leq (N-1) \\ 0 & \text{elsewhere} \end{cases}$$

The Kaiser Window Function (4)

$$W[n] = \begin{cases} \frac{I_0\left\{\beta \left[1 - \left(\frac{n}{N}\right)^2\right]\right\}^{1/2}}{I_0(\beta)} & 0 \leq n \leq (N-1) \\ 0 & \text{elsewhere} \end{cases}$$

where $I_0(x)$ is the zero-order Bessel function of the first kind, β is an adjustment parameter and $I_0(x)$ is calculated using the rapidly converging series:

$$I_0(x) = 1 + \sum_{k=1}^{\infty} \left[\frac{1}{K!} \left(\frac{x}{2} \right)^k \right]^2 \quad (5)$$

20 terms are sufficient for a very close approximation to $I_0(x)$.

The β parameter is used to 'tune' the Kaiser window function and produce a matched filter correlation with the desirable characteristics of a high peak-to-sidelobe ratio (PSR). The optimal value of the β parameter to maximise the PSR for the "chirp" matched filter was calculated to be $\beta=7.2$.

The Kaiser window with $\beta=7.2$ resulted in a marginally improved PSR, with no AWGN, compared with the Hamming window. However, its performance deteriorated with levels of AWGN above zero, as shown in Figure 1. Hence, the Kaiser window function proved to have no significant advantage over the Hamming window; thus attention was focused on the rectangular, Hamming and Blackman windows.

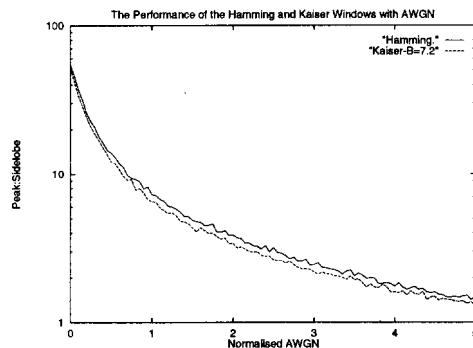


Figure 1 The Performance of the Hamming and Kaiser Window Functions with AWGN

The means of the parameter values calculated using a series of chirp signals with input phase shifts of 0.1 degree are shown in the table below.

Window Function	Mean Peak	Mean RMS Width (mS)	Mean PSR
Rectangular	128.0	0.337	4.79
Hamming	69.1	0.505	70.8
Blackman	53.8	0.641	67.6

Table 1 The Important Window Function Parameters

The results in Table 1 follow the expected pattern: that is, the higher the order the of the window function, the greater the chirp weights are tapered at the beginning and end; thus the smaller the resultant coherent gain. The RMS width of the main lobe conversely increases - reducing the resolution. But the PSR, which is crucial to identify unambiguously attenuated multi-path

propagation is a maximum with the Hamming window function.

The relative performance of the window functions to Additive White Gaussian Noise (AWGN) is critical because HF radio channels contain large quantities of signal noise from other users and naturally occurring sources, which can severely impair the systems' ability to determine ionospheric structures. In order to maximise the signal energy and reduce the effects of narrow band noise, all of the available channel bandwidth should be utilised for the chirp detection. The rectangular window achieves this; thus it is the least affected by AWGN. Figure 2 shows the performance of the matched filter with the considered window functions and AWGN.

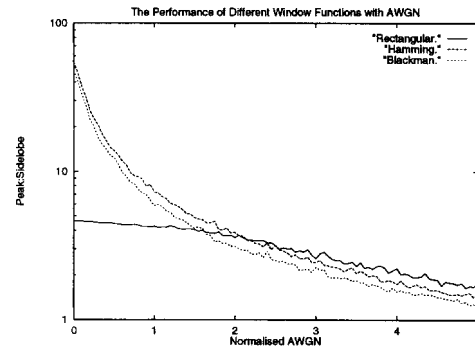


Figure 2 The Performance of Different Window Functions with Band limited AWGN

The Hamming window is superior to both the Blackman window and Kaiser window in terms of PSR with all levels of AWGN. However, the rectangular window out-performs them both with a normalised AWGN above 2. Therefore, it would be beneficial to recognise channels with high levels of background noise, to facilitate the use of a Rectangular window function. The parameters for optimal recovery of the chirp signal have now been discussed. It is now intended to consider the enhancement of the ionogram display.

MEDIAN FILTERING

Random noise occurring in the channel impulse responses is unlikely to occur at similar times on adjacent channels; in contrast, the features of interest (i.e. propagation modes due to ionospheric layers) are probable at similar times across neighbouring channels. The use of a median filter removes the random point noise from the ionogram before the peak detection algorithm is applied. The standard median filter [5] replaces extreme values in the channel impulse response with the middle or median value of an ascending order sort, of its own and neighbouring data points, according to the following algorithm.

$$\begin{array}{ccc} A & D & G \\ B & E & H \\ C & F & I \end{array}$$

$$E' = \text{median}(A, B, C, D, E, F, G, H, I) \quad (6)$$

where D, E, F are data points from channel n, A, B, C are adjacent data points from channel n-1 and G, H, I are adjacent data points from channel n+1.

The standard median filter, described above, effectively removes invalid points from the ionogram. However it also removes some points along the ionospheric layers, which are of interest.

A hybrid class of median filters exists which attenuate point noise but do not remove fine detail such as faint lines. An example being a two level linear-median hybrid filter termed "2LH+" [6].

$$\begin{array}{ccccc} E & - & D & - & C \\ - & E & D & C & - \\ F & F & A & B & B \\ - & G & H & I & - \\ G & - & H & & I \end{array}$$

(7)

A 5x5 region is used and the positions marked with a '-' are ignored.

$$A' = \text{median}(A, \text{median}(A, B, D, F, H), \text{median}(A, C, E, G, I))$$

In practice, the "2LH+" hybrid median filter in practice caused additional invalid points to be plotted, thus proving unsuccessful in enhancing ionogram quality.

LOW-PASS SPATIAL FILTERING

Low-pass filtering is the removal of high spatial frequency components. It is possible to accomplish this type of operation [7] in the spatial domain by convolution with the Fourier transform. For a low-pass filter to have a sharp cut-off, the transform in the spatial domain must be oscillatory [7]. The disadvantage of this algorithm is that it produces distorting halos around significant features. Marr and Hildred [8] suggest that the best types of filter to apply are well behaved (non-oscillatory) in the spatial and frequency domain. Gaussian filters satisfy this criterion; they have identical forms in the spatial and frequency domains. In 1-dimensional form they can be represented by;

$$\begin{aligned} f(x) &= [1/(2\pi\sigma^2)^{1/2}] \exp[-x^2/(2\sigma^2)] \\ F(\omega) &= \exp(-\sigma^2\omega^2/2) \end{aligned} \quad (8)$$

Hence, spatial convolving operators, which suppress noise by low-pass filtering should approximate to a Gaussian profile. One of the most common masks chosen for simplicity of computation, rather than its closeness to a Gaussian profile, is:

$$E' = \frac{1}{9} \begin{bmatrix} (1 \times A) & (1 \times D) & (1 \times G) \\ (1 \times B) & (1 \times E) & (1 \times H) \\ (1 \times C) & (1 \times F) & (1 \times I) \end{bmatrix} \quad (9)$$

Another mask chosen which approximates more closely to a Gaussian profile is:

$$E' = \frac{1}{16} \begin{bmatrix} (1 \times A) & (2 \times D) & (1 \times G) \\ (2 \times B) & (4 \times E) & (2 \times H) \\ (1 \times C) & (2 \times F) & (1 \times I) \end{bmatrix} \quad (10)$$

Due to the nature of this task (of enhancing ionograms) the relative merits of the various techniques can not be quantified exactly but they have been graded, through inspection of results on recorded impulse response data.

RESULTS

Low-pass spatial filtering gives better results than median filtering and has the advantage of interpolating the lines which represent ionospheric layers. An example of a standard output digital ionogram is shown in Figure 3 and the enhanced version which has been subject to spatial filtering is shown in Figure 4. The enhancement of longitudinal phenomena and the attenuation of vertical (channel specific) features, which results in the improved definition of ionospheric layers, prompted investigations with custom convolution masks. One which achieved good results is:

$$C' = \frac{1}{5} [(1 \times A) \quad (1 \times B) \quad (1 \times C) \quad (1 \times D) \quad (1 \times E)] \quad (11)$$

This elongated mask enhances ionospheric layers which run longitudinally in the ionogram and severely attenuates isolated noise or channel-specific noise. An important implementation aspect that has not yet been mentioned, is that the software threshold, calculated for each channel, must be averaged over the adjacent signal processed channels to maintain channel noise level correspondence.

CONCLUDING REMARKS

The enhancement process of separating the layer structures from the noise does modify the measured channel impulse responses. This is a performance criterion trade-off for the isolation of the features of interest. The ionospheric layers can then be classified and the modal structure and MUF and LUF parameters extracted for frequency management purposes. The real-time determination of these fundamental propagation parameters enables the optimisation of frequency selection and gives the ability to forecast likely changes from past data.

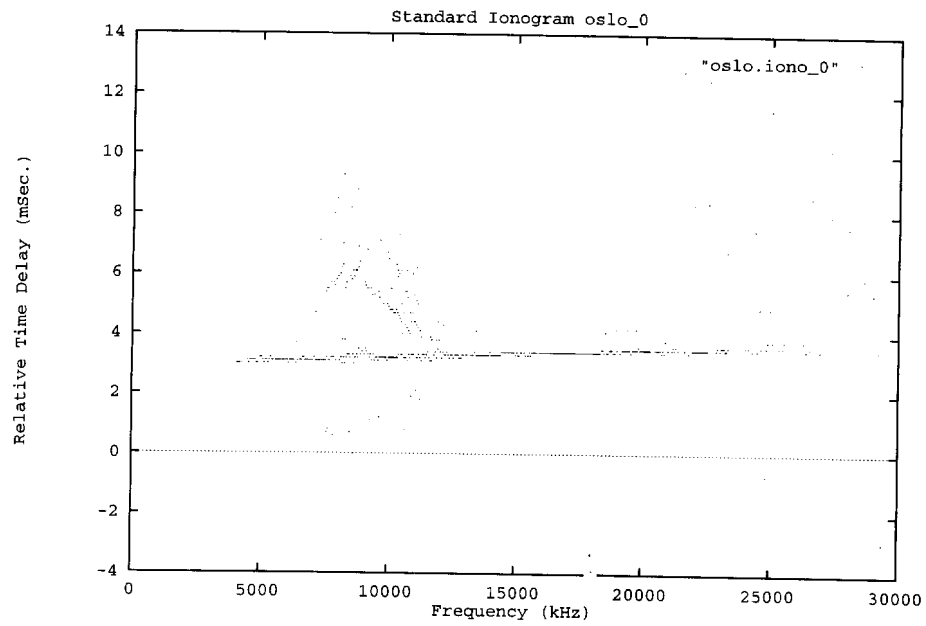
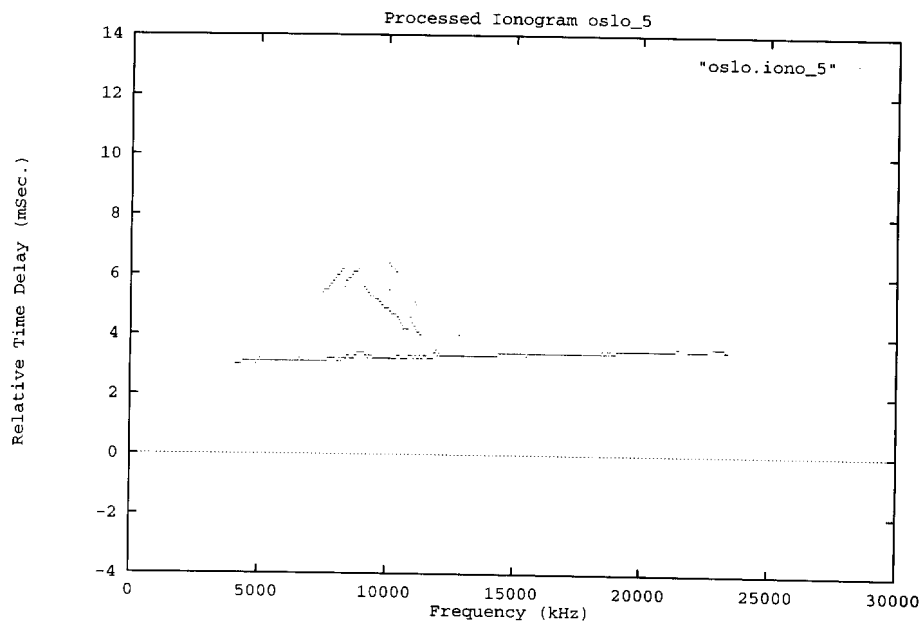
The system under development uses the same HF radio terminal for communication and ionospheric measurement. The generic system will adaptively select the best transmission frequencies for current operation and predicted future reliability based on ionospheric structures and their movement.

ACKNOWLEDGEMENTS

The support of the Engineering and Physical Sciences Research Council (EPSRC), Siemens-Plessey Systems (Christchurch) and the Department of Electronic Engineering, University of Hull, are gratefully acknowledged by the authors.

REFERENCES

1. BARRY, G.M., 1966, 'Oblique 'chirp' sounding', AGARD, Conf. on 'Ionospheric oblique radio propagation at frequencies near the lowest usable frequency', Leicester.
2. GALLAGHER, M. & DARNELL, M., 1991, 'An economic ionospheric sounding system using standard HF radio system elements', *HF Radio Systems and Techniques*, No. 339, pp 269-274.
3. HARRIS, F., 1978, 'On the use of windows for harmonic analysis with the discrete Fourier transform', *Proceedings of IEEE*, Vol. 66, No.1, pp. 51-84.
4. BAHER, H., 1990, "Analogue and Digital Signal Processing", John Wiley & Sons Ltd, Chichester, pp 57, 328.
5. DAVIES, E.R., 1990, "Machine Vision", Academic Press Limited, Cambridge, pp. 44-76.
6. NIEMINEN, A. HEINONEN, P. and NEUVO, Y., 1987, 'A new class of detail preserving filters for image processing', *IEEE Trans. Pattern Anal. Mach. Intell.* 9, pp. 74-90.
7. ROSIE, A.M., 1966. "Information and Communication Theory", Blackie, London.
8. MARR, D. and HILDRETH, E., 1980, "Theory of Edge Detection", *Proc. R. Soc. B207*, London, pp. 187-217.

Appendix A An example of ionogram enhancement**Figure 3** A Standard Ionogram (Oslo to Cobbett Hill 10am 8/8/90)**Figure 4** A Low Pass Spatial Filtered Ionogram (Oslo to Cobbett Hill 10am 8/8/90)